CHAPTER II
THEORY AND LITERATURE REVIEW

Hydrogen damage has been observed in petroleum refining and petrochemical equipment used in the environment with high hydrogen pressures at elevated temperatures. This damage is caused by the entry of hydrogen into steel. Most petroleum refining and petrochemical plant operations involve hydrocarbon gases and strong acids or caustics that are often at elevated temperatures and pressures. The many metals and alloys that are available are susceptible to hydrogen damage along with the typical damage inducing conditions. The Nelson curves, which are based on services experience, were suggested to define the operating limits for steels used in hydrogen service to avoid hydrogen damage. The curve is shown schematically in Figure 2.1. It is suggested that equipment should be operated near or below the curve. Even for particular steel under the desired conditions, the exposure of hydrogen can cause deterioration of the mechanical properties of the steel.

Hydrogen cracking in pipeline steels in the United States was first reported in 1954. In 1974, the major failure with a sour-gas pipeline in Saudi Arabia occurred within a few weeks of startup and affected a length of about 10 km(Eleboujdaini,2000). The reactor feed line and outlet line of a coker distillate hydrotreating unit which used C-0.5Mo as the steel piping was found to undergo decarburization and internal fissuring/cracking (Hennie de Bruyn, 2004). Water-wall tube failures in a coal and oil-fired boiler in service for 12 years have been caused by localized corrosion and hydrogen damage(Hahn,1993; API, 2004).

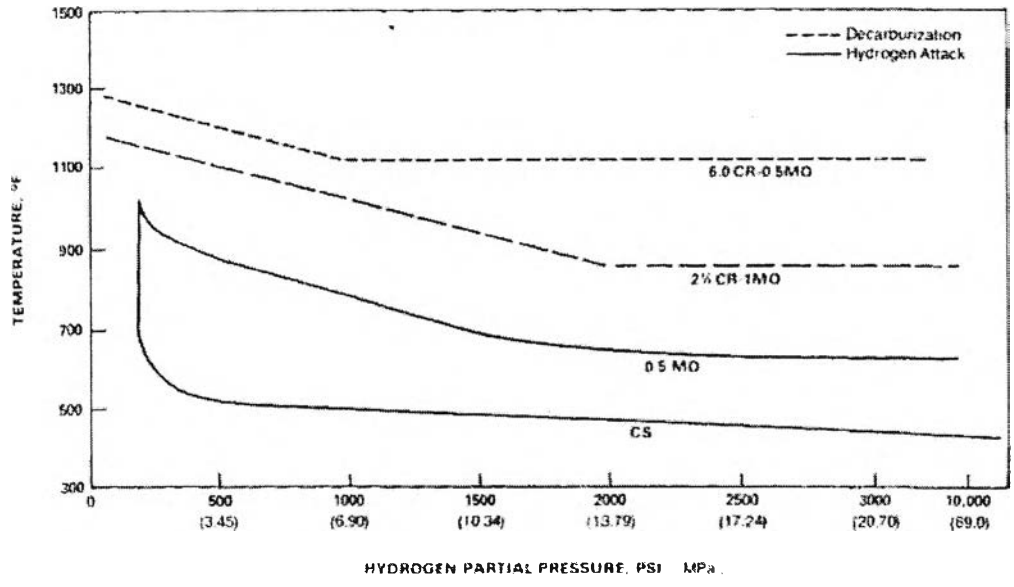

Figure 2.1 The Nelson Curve with steels in high temperature hydrogen service (API, 2004).

A very common failure in fossil boiler tubes is hydrogen damage/attack (Speidel and Atrenes,1984; Metals-handbook,1987). It results from acid corrosion either due to condenser leaks allowing enters of chloride or improper solutions. The atomic hydrogen generated by corrosion reactions diffuses into the metal and reacts with carbon present in the iron carbides to form methane bubble. Reduction in carbon content leads to decarburization. The large methane molecules trapped produce very high delocalized stress leading to micro fissures which can form cracks.(Dayal and Parvathavarthini, 2003)

Antonio (1993) reported irreversible hydrogen attack occurred in several high pressure steam pipe which were in service for as long as 25 years as shown in Figure 2.2. Parvathavarthini (1995) noted that proper post weld heat treatment (PWHT) is not performed after welding, corrosion generated hydrogen is likely to cause failure as shown in Figure 2.3.

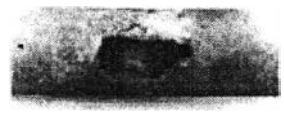

Figure 2.2 High pressure steam pipe containing blow out window fracture (Antonio, 1993).

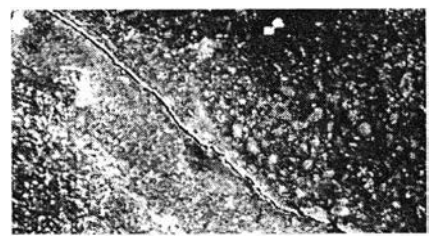

Figure 2.3 Hydrogen-induced cracking in 9Cr-1Mo steel due to repair welding without PWHT (Parvathavarthini, 1995).

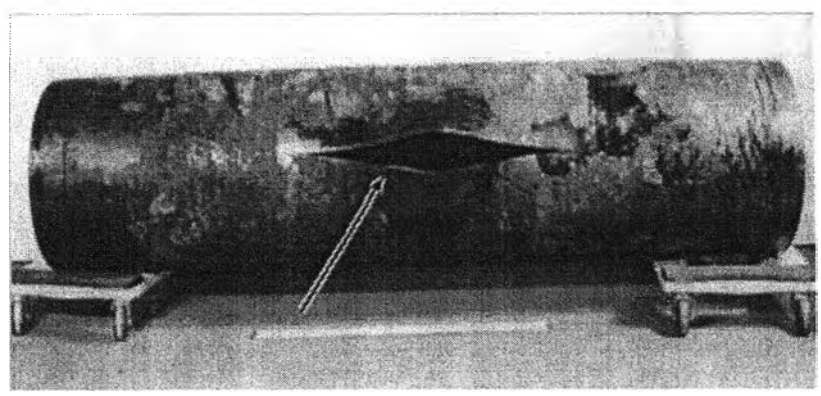

Figure 2.4 Pipeline rupture caused by hydrogen embrittlement (http://www.ntsb.gov).

Several major corrosion problems at refineries have been associated with carbon steel parts and piping that do not fall within specified material content guidelines. Over the years the refining industry has found that corrosion increases dramatically in hydrofluoric acid (HF) alkylation units where carbon steel piping and components contain elevated levels of residual elements–Cr, Ni and Cu.(Mears, 2009)

Mousavinejad (2005) also mentioned sources of hydrogen causing embrittlement have been encountered in the making of steel, in the drilling processes, machining or forming, in welding, in the processes of corrosion or rusting during

storage and transportation, in chemical cleaning or pickling operations, in electrocleaning operation, in electroplating and electroless plating operations, and in the process of cathodic protection.

2.1 Hydrogen Damage

The likelihood of hydrogen induced materials damages depends on the rate of hydrogen uptake, the hydrogen concentration in the material, the susceptibility of the material to hydrogen induced cracking and finally the rate of hydrogen effusion the material (Schmitt and Ma, 2008).

Hydrogen can be present in contact with an external surface in the form of a molecule, a dissociated molecule or atom, or a component of complex molecule, such as H_2S or CH_3OH or contact with an internal surface in the form of an atom or molecule (Nelson, 1983). Hydrogen dissolves in metals as an atom rather than as molecule hydrogen. Thus, adsorption and desorption of hydrogen requires the presence of atomic hydrogen on the metal surface. The atomic hydrogen forms on the metal surface, when exposed to a gaseous hydrogen environment, by dissociation of hydrogen molecules

Hydrogen damage in industry equipments takes many forms. The ASM material Handbook lists five specific types of hydrogen damage to metal and alloys. These types are:

1) Cracking from Hydrogen-induced blistering
2) Cracking from precipitation of internal hydrogen
3) Cracking from hydride formation
4) Hydrogen attack
5) Hydrogen embrittlement

The mechanisms for each of these failure modes are described below.

2.1.1 Hydrogen-Induced Blistering

Hydrogen-induced blistering occurs during or after hydrogen has been absorbed by the metal. The atomic hydrogen collects at the extraordinary sites, which

include the interface between inclusions and the metallic matrix, in the metal. The collecting hydrogen recombines to form a pressure at the inclusion-matrix interface and then precipitates as molecular hydrogen. The pressure will depend on the concentration of absorbed hydrogen in the metal, the trapped hydrogen, the dissolved hydrogen and the temperature. If there is sufficient hydrogen absorbed in the metal, the pressure will become high enough to plastically deform the surrounding metal. If the deformation is sufficient, a blister will form at the external surface above the inclusion.

Blistering is frequently found in low-strength steels. Its formation needs the metal to contain inclusions or other internal surfaces where hydrogen can accumulate. The metal absorbs the hydrogen either prior or during service.

2.1.2 Cracking From Precipitation of Internal Hydrogen

The damage from the precipitation of internal hydrogen has been termed fisheyes, shatter cracks and flakes. These are damages in forging, weldments, and castings. They are charged to hydrogen during melting operations. The melt has a higher solubility for hydrogen than the solid alloy. During the cooling process from the melt, hydrogen diffuses to and precipitates in voids because the lower temperature reduces the solubility of hydrogen in the solid metal. In case of Welding process, hydrogen in atomic form gets absorbed in the weld metal pool, and then can rapidly diffuse to the heat affected zone at ambient temperature and can cause cold cracking even before post weld heat treatment is performed.

2.1.3 Cracking from Hydride Formation

Hydride formation produces failure in magnesium, tantalum, niobium, vanadium, uranium, zirconium, titanium and their alloys, as well as many other less common metals and alloys. The fundamental structures of these metals are quite different. They will form hydride when the hydrogen concentration exceeds a certain level. The hydrides are typically low density, brittle compounds whose presence degrades the ductility of the metal. The degradation of mechanical properties and the cracking of these metals can precipitate as metal hydride phases.

2.1.4 Hydrogen Attack

Hydrogen attack is the damage that cannot be irreversible even after the hydrogen is removed, as by a thermal outgassing treatment. Hydrogen attack may occur when steels are exposed to hydrogen at elevated temperatures and pressures; for plain carbon steels this means above approximately 200°C and 25 atmospheres. Thus, hydrogen attack is of interest in all industries where hydrogen-bearing fluids are processed.

The basic process leading to hydrogen attack is a reaction between the highly mobile hydrogen and carbon in the steel, to form methane. The methane cannot mobile and it collects in bubbles, usually in the grain boundaries, which grow as the reaction continues. The dissolved carbon is consumed, and then the iron carbide dissolves to provide the carbon required for the methanation reaction. High methane pressures may develop in the bubbles. The microstructural damage caused by hydrogen attack is clearly irreversible (Johnson, 1982).

The mechanical properties of the steel deteriorate during hydrogen attack for two reasons. First, the grain boundaries are weakened by the methane-filled bubbles. Second, the dissolution of the iron carbides removes a primary source of the strength of the steel.

2.1.5 Hydrogen Embrittlement

Hydrogen embrittlement is dependent on many variables such as temperature, pressure, level and type of stresses, environment, physical and mechanical properties of bulk materials, type and concentration of impurities in the metal, thermomechanical history, hydrogen diffusion rate and surface conditions (Dayal and Parvathavarthini, 2003).

Hydrogen embrittlement (HE) is also caused by penetration of atomic hydrogen into the crystal structure of metal. Molecular hydrogen formed at those sites builds up pressure causing the rupture of the inter-atomic bonds, which results in a loss of ductility and decreases the cohesive strength ; the voids and blisters are formed voids and leads to the formation of cracks on the material (Dinu Gheorghe Matei, 1999).

Hydrogen embrittlement is the reversible reduction in ductility, and often fracture strength of steels charged or exposed to hydrogen at temperature around 300 K. The original ductility is restored if the hydrogen is removed by thermal treatment. Hydrogen transport under embrittlement may be influenced and controlled by parameters other than the lattice diffusivity. Two important factors are hydrogen trapping at special sites in the microstructure, which hinders transport, and dislocation motion during plastic straining, which enhances transport. Hydrogen trapping near 300 K has long been reflected in effective hydrogen diffusivity measured by permeation techniques (Johnson, 1982).

Table2.1 Classifications of processes of hydrogen degradation of metals

	Hydrogen Induced Blistering	**Cracking from precipitation**	**Cracking from hydride formation**	**Hydrogen attack**	**Hydrogen embrittlement**
Material	Steels, Copper, Aluminum	Steels(forgings and castings)	V, Nb, Ta, Ti, Zr, U	Carbon steels and Low-alloy steel	Steels, nickel-base alloys, stainless steel, titanium alloys
Source of Hydrogen	Hydrogen Sulfide corrosion	Water vapor reacting with molten steel	Internal hydrogen from melt; corrosion, electrolytic charging welding	Gaseous H_2	Gaseous H_2
Operational conditions	0.2 to 1 x 10^8 N/m^2	Precipitation of ingot cooling	10^5 to 10^8 N/m^2 (15-15000 psi)	Up to 10^8 N/m^2	$10^{-6}$to 10^8 N/m^2(10^{-10} to 10^4 psi gas pressure)
	0-150 °C		Hydrogen activity must exceed solubility limit near 20°C	200-595 °C	-100 to 700 °C Most severe near 20°C

2.2 Hydrogen Damage Prevention Methods

There are several studies mentioning the traditional methods to minimize the occurrence of hydrogen damage. They consist of (1) Post-process heating of the metal to allow hydrogen off-gassing, (2) Practice cleaning, for example acid cleaning, and processing techniques that minimize hydrogen production and absorption (3)

Inhibitors or coatings that can be applied to reduce corrosion (4) Metals and alloys with less susceptible to hydrogen damage, and (5) the process operated below the metal's Nelson Curve.

2.3 Permeation of Hydrogen and Fundamental Law of Diffusion

Hydrogen molecules permeate through steels involving its entrance at one surface and its exit at the other surface of the specimen as shown in Figure 2.5. The gaseous hydrogen molecule can enter only at sites that are not occupied by other adsorbed molecules. Only the molecules that have adequate energy will be adsorbed, otherwise the molecule will be desorbed again.

Shanabarger and co-workers mentioned at the entrance side of the material molecular hydrogen adsorbs and desorbs from a precursor state, H^*. Dissociation and recombination occur between the precursor state (physisorbed) and the chemisorbed state, H. The chemical bonds are not broken in the physisorption state. Van der waals force couples the molecule to the surface which does not dissociate. In the chemisorbed state, the adsorbed molecule shares an electron with the substrate. The bond is between the atomic hydrogen and the oxide surface. From the chemisorbed state, hydrogen can go into the bulk of material establishing a subsurface hydrogen concentration, C_H.

Depending on the driving pressure of hydrogen and the temperature of the membrane, the permeation rate can be surface limited, bulk limited or a combination of both. When the process is bulk limited, the hydrogen transport is controlled by the passage of hydrogen ions through the lattice, dislocations, grain boundaries and triple junctions or other defects in the system. Surface limited transport on the other hand is controlled by parameters affecting surface adsorption, dissociation and recombination (Mousavinejad, 2005).

This model accounts for the presence of surface films on both input and output side of the specimen. The seven steps consist of:

1) Adsorption of the hydrogen molecule on the oxide surface.
2) Dissociation of the absorbed molecule on the surface.
3) Permeation of dissociated atoms through the surface oxide film.

4) Permeation of the atoms through the metal.
5) Permeation of the atoms through the oxide film on the output side.
6) Recombination of the atoms to form H_2 molecules.
7) Desorption of the recombined H_2 molecule.

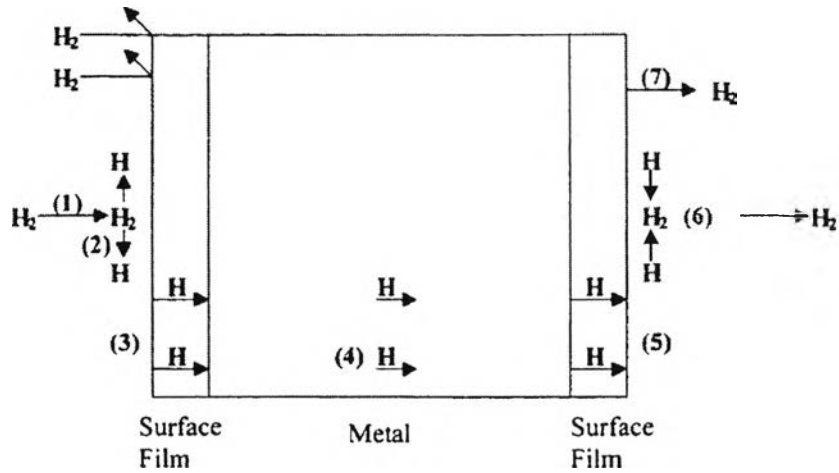

Figure 2.5 Seven steps of hydrogen permeation (Stone,1981).

The above stages may be characterized formally by the respective resistances: hydrogen entry R_{in}, inside surface $R_{surf,in}$, diffusion R_{diff}, outside surface $R_{surf,out}$ and exit R_{out} resistances. In the case that a metal membrane is coated with a thin layer of palladium, the hydrogen diffusion in the palladium layer resistance also should be considered as R_{pd}. The hydrogen permeation rate should be inversely proportional to the sum of these resistances:

$$\text{Permeation rate} \sim \frac{1}{R_{in} + R_{surf,in} + R_{diff} + R_{Surf} + R_{out,out}} \quad (1)$$

When the palladium is applied on the outside surface of membrane, the permeation rate becomes

$$\text{Permeation rate} \sim \frac{1}{R_{in} + R_{surf,in} + R_{diff} + R_{Pd} + R_{out}} \quad (2)$$

The diffusion resistance is proportional to L/D, where L is the membrane thickness of the membrane and D is the diffusion coefficient of hydrogen in the membrane. Since palladium has a relatively high diffusivity and the palladium layer is much thinner than the studied membrane so that the palladium coating resistance R_{Pd} is negligible ($R_{Pd} << R_{diff}$) Thus the equation reduces to

$$\text{Permeation rate} \sim \frac{1}{R_{in} + R_{surf,in} + R_{diff} + R_{out}} \quad (3)$$

Usually, the membrane employed are of such thickness that $R_{diff} >> R_{in}$, which means that the permeation rate is determined by the diffusion rate in the membrane.

It has been established that the rate of hydrogen entry in a metal is affected by the nature of metal or alloy, its composition, thermal mechanical history, temperature, pressure, presence of surface layers and/or presence of impurities (Matei, 1999) .

An important aspect of hydrogen behavior is the substantial enhancement of absorption in the presence of specific compounds. These compounds such as S^{2-}, HS^-, H_2S, As etc. hinder the recombination of hydrogen atom on the metallic surface and therefore enhance the absorption reaction. These compounds are usually referred to as poisons and concentrations have an effect in increasing hydrogen into metals and alloys even they are in low concentration (Store, 2006).

Inhibitors of hydrogen entry into metals and alloys function by adsorption as a thin protective film onto the surface of the metal or adding inhibitor to change the chemical properties of the substrate. Hydrogen coverage on the surface is decreased (Matei,1999). For example, Zn, Bi, Pb inhibits the hydrogen discharge reaction and reduces the degree of hydrogen entry (Duarte, 1997).

The presence of oxide films formed on the metallic surfaces is a barrier for H absorption and is hindering the hydrogen passage through the interface.

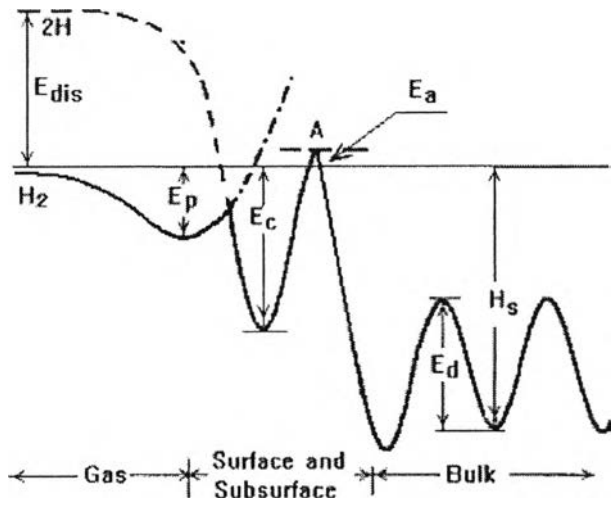

Figure 2.6 Potential energy curves for molecule and atom of hydrogen on metal surface. E_{dis}–energy of molecular dissociation, E_p–heat of physisorption, E_c–heat of chemisorptions, E_a–activation energy for bulk uptake, E_d–diffusion activation energy, H_s–heat of solution (Liu and Shi, 2004).

Liu et al.(2004) mentioned the hydrogen molecule with the metal surface is a typical chemical process. The dissociation energy for the hydrogen molecule, E_{dis}, typically 432 kJ $mol^{-1}$is exceeded by the chemisorptions energy ,E_c ,which varies between 500 and 600 kJ mol^{-1}, depending on the metal involved. After being chemisorbed into the energy well E_c, H atoms still with considerable vibration amplitude will jump over the top point A and become absorbed in the bulk. When the surface barrier potential E_a is higher, neither penetration nor diffusion occurs. The barrier is lower so it is equal to the value of the heat of solution H_s, H atoms can directly transfer into the bulk solution phase. They also noted when the surface and subsurface layer cannot dissolve hydrogen anymore, equilibrium between chemisorptions, surface penetration, and diffusion into the bulk is reached and hydrogen uptake in the metal is saturated.

2.3.1 Steady State Behavior

The steady-state situation may be associated with the passage of hydrogen through a membrane. If conditions are maintained constant, the permeation rate becomes constant after sufficient time (Matei, 1999). The permeation rate of

hydrogen passing through a specimen will be established by the diffusivity and the difference between the hydrogen concentrations at the inlet side and the outlet side. Under the assumption that there are no surface effects on both sides of the specimen, the hydrogen surface concentration will be equal to the solubility limit for hydrogen in that metal (Stone, 1981). When the steady-state condition is reached, the concentration gradient of hydrogen through the specimen will be linear.

The permeability of a material determines the flow rate of hydrogen through a specimen once steady state flow is attained. The diffusivity or diffusion coefficient, which refers to the rate of movement of individual hydrogen atoms, determines the time necessary to reach steady state flow. The solubility refers to the dissolved hydrogen concentration per unit of applied pressure of hydrogen. These parameters are related through the expression (Mousavinejad, 2005):

$$\text{Permeability} = \text{Diffusivity} \times \text{Solubility} \tag{4}$$

The effect of temperature on the hydrogen permeability through the metals can be described by an Arrhenius equation as follows:

$$\Phi = \Phi_0 \exp\left(\frac{-E_P}{RT}\right) \tag{5}$$

where Φ = Permeability, permeation rate

Φ_0 = Temperature independent factor for permeability

E_p = Activation energy for permeation

R = Universal gas constant

T = Absolute temperature

In the case of the diffusion coefficient (D) as a function of temperature, the Arrhenius's Law is often found to give a good prediction as shown in Equation below:

$$D = D_0 \cdot e^{\frac{-E_A}{RT}} \tag{6}$$

where D = Diffusion coefficient

E_A = Activation energy for diffusion

T = Absolute temperature

R = Ideal Gas Constant

Permeability and diffusivity are thermally activated processes, thus they feature Arrhenius-type dependence on temperature and, like solubility, can be expressed in the general form

$$S = S_0 \exp\left(\frac{-E_S}{RT}\right) \tag{7}$$

where S = Solubility

E_S = Activation energy for solution in metal

T = Absolute temperature

R = Ideal Gas Constant

The typical method for determining permeability, diffusivity, and solubility assumes that hydrogen transport is governed by diffusion in the bulk. The surface oxide layers are assumed to give small resistance.

2.3.1.1 Planar Membrane

In general, permeability of hydrogen and its isotopes is defined as the steady-state transport of atoms through a material that supports a pressure difference. Assuming steady state, a semi-infinite plate, and *Fick's first law* for diffusion.

$$J = -D\frac{\partial C}{\partial x} \tag{8}$$

where J = Diffusion flux $\left(\text{mol}/\text{m}^2.\text{s}\right)$

D = Diffusion coefficient or diffusivity $\left(\text{m}^2/\text{s}\right)$

C = Concentration of the diffusing $\left(\text{mol}/\text{m}^3\right)$

x = Coordinate chosen perpendicular to the reference surface (m)

After adsorption and dissociation hydrogen is dissolved from the atmosphere by absorption according to:

$$H_2\,(gas) = 2H\,(dissolved) \qquad (9)$$

And the concentration of dissolved gas (or solubility) ,C_H at equilibrium with a gas pressure P_H follows '*Sievert's Law*'

$$C_H = k_S\sqrt{P_{H_2}} \quad mol/m^3 \qquad (10)$$

where P_{H_2} = Pressure of the hydrogen gas in the environment

C_H = Concentration of dissolved atomic hydrogen in the metal

k_s = Sieverts constant

Oriani et al. (1994) noted that hydrogen dissolved in metals at low concentrations exhibits a linear relation between the concentration and the half power of the pressure, P, of the molecular gas. This is proof that hydrogen dissociates when it enters the metal.

The derivation of *Sievert's Law* also assumes that the surface coverage of hydrogen at both the feed and permeate sides of the membrane is in equilibrium with the respective fluid phases, and that the adsorption equilibrium constant is the same on both sides.

From the numerous measurements of Sieverts and others, it was shown that the solubility of gases having diatomic molecules is proportional to the square of the hydrogen gas pressure. According to Henry's law, if the molecular condition of the hydrogen gas in the metal is the same as in the gaseous state, the solubility should be proportional to the hydrogen pressure.

Permeability becomes important when the surface concentrations of the gas are not known. Since inlet and outlet pressure are easily measured, pressure is substituted into *Fick's first law*. In the case of diatomic molecules such as H_2, which dissociates before dissolution in the metal, a modification of *Sievert's law* is needed ($C_H = k_S\sqrt{P_{H_2}}$). This is then used to convert *Fick's law* into the usable equation.

$$J = \frac{-D(C_2 - C_1)}{l} = \frac{-Dk_s(P_{H_2,2}{}^{1/2} - P_{H_2,1}{}^{1/2})}{l} \quad (\text{mol of gas})\ m^{-2}s^{-1} \qquad (11)$$

where J is the rate of gas permeation/unit area of material of thickness l; $P_{H_2,2}$ and $P_{H_2,1}$ are the gas pressures on the exit and entry sides respectively; D is the diffusion coefficient of the material(with units: m^2/s) and k_s is the Sieverts constant for the material (with units: mol $m^{-3}Pa^{-0.5}$).

The product Dk_s is sometimes referred to as Φ, the permeation coefficient or permeability of the material (the units of Φ are: mol m^{-1} s^{-1} $Pa^{-0.5}$). In the particular case where $P_{H_2,2}$ is negligible. Thus, the equation reduces to

$$J = \frac{\Phi P_{H_2,1}^{1/2}}{l} \quad \text{mol m}^{-2}\text{s}^{-1} \tag{12}$$

D, k_s and Φ are found to vary in the Arrhenius manner with temperature

2.3.1.2 Hallow Cylindrical Membrane (Huang and Yen, 2002)

Consider a long circular cylinder in which diffusion is everywhere radial. Concentration is then a function of radius r and time t only, and the diffusion equation becomes

$$\frac{\partial C}{\partial t} = \frac{1}{r}\frac{\partial}{\partial r}\left(rD\frac{\partial C}{\partial r}\right) \tag{13}$$

where C = Concentration [mol m^{-3}]

t = Time [s]

D = Diffusivity [m^2 s^{-1}]

r = radius [m]

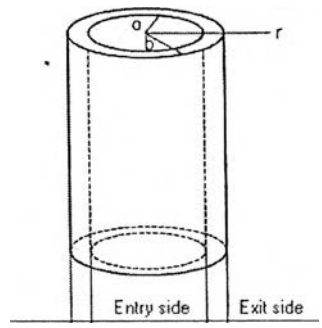

Figure 2.7 Schematic representation of diffusion in hollow cylinder (Huang and Yen, 2002).

If the specimen has inner and outer radii of a and b as shown in the Figure 2.7, and the diffusion coefficient is constant, the equation describing the steady-state condition is

$$\frac{\partial}{\partial r}\left(r\frac{\partial C}{\partial r}\right) = 0, \quad a < r < b \tag{14}$$

The boundary conditions become

$$t \leq 0, \quad a < r < b, \qquad C = 0$$
$$t > 0, \qquad r = a, \qquad C = C_0$$
$$t > 0, \qquad r = b, \qquad C = 0$$

Thus, the solution is

$$C = -\frac{C_o \ln\left(\frac{r}{b}\right)}{\ln\left(\frac{b}{a}\right)} \tag{15}$$

And the flux of the steady state at r=b is

$$J_\infty^b = -D\left(\frac{dC}{dr}\right)_{r=b} = \frac{DC_0}{b\ \ln\left(\frac{b}{a}\right)} \tag{16}$$

2.3.2 Time Dependent Behavior

2.3.2.1 Planar Membrane

When the concentration within the diffusion volume changes with respect to time, non-steady state diffusion occurs. *Fick's second law* applies assuming that the diffusion takes place in a homogeneous and isotropic medium and that the diffusion coefficient D does not depend on the concentration C.

$$\frac{\partial C}{\partial t} = D\frac{\partial^2 C}{\partial x^2} \tag{17}$$

where C = Concentration [mol m^{-3}]

t = Time [s]

D = Diffusivity [m^2 s^{-1}]

x = Position [m]

It can be derived from the Fick's First Law and a mass balance

$$\frac{\partial C}{\partial t} = -\frac{\partial}{\partial x}J = \frac{\partial}{\partial x}\left(D\frac{\partial}{\partial x}C\right) \tag{18}$$

Assuming the diffusivity (D) to be a constant one that can exchange the orders of the differentiation, and multiplying by the constant

$$\frac{\partial}{\partial x}\left(D\frac{\partial}{\partial x}C\right) = D\frac{\partial}{\partial x}\frac{\partial}{\partial x}C = D\frac{\partial^2 C}{\partial x^2} \tag{19}$$

2.3.2.2 Hallow Cylindrical Membrane (Huang and Yen, 2002)

The example of non-steady state diffusion is given by Carslaw and Jaeger. They give the solution to the problem of diffusion into a hollow with initial concentration $f(r)$ and the two surfaces $r = a$ and $r = b$ kept at zero concentration. The general solution is

$$C = \frac{\pi^2}{2}\sum_{n=1}^{\infty}\frac{\alpha_n^2 J_0^2(a\,\alpha_n)}{J_0^2(a\,\alpha_n) - J_0^2(b\alpha_n)}\exp(-D\alpha_n^2 t)\,U_0(r\alpha_n)\int_a^b r\,f(r)\,U_0(r\alpha_n)\,dr \tag{20}$$

$$t \le 0, \quad a < r < b, \qquad C = C_0\frac{\ln\left(\frac{b}{r}\right)}{\ln\left(\frac{b}{a}\right)}$$

$$t > 0, \qquad r = a, \qquad C = 0$$

$$t > 0, \qquad r = b, \qquad C = 0$$

After substituting the boundary conditions into general equation of this case, the normalized flux is given by

$$\frac{J_t^a}{J_\infty^a} = \pi \ln k \sum_{n=1}^{\infty}\frac{J_0(a\alpha_n)J_0(ka\alpha_n)}{J_0^2(a\alpha_n) - J_0^2(ka\alpha_n)}\,exp[-(a\alpha_n)^2\tau] \tag{21}$$

where a = inner radius of cylinder

b = outer radius of cylinder

C = concentration in cylinder

C_0 = concentration at input surface

D = diffusion coefficient

J_t^a = permeation flux of transient state at r=a

J_∞^a = permeation flux of steady state at r=a

J_0 = Bessel function of the first kind, order 0

k = ratio of b to a

τ = Dt/a^2

α_n = the positive roots of $J_0(a\alpha)Y_0(b\alpha_n) - Y_0(a\alpha)J_0(b\alpha) = 0$

Table2.2 Roots of $J_0(a\alpha_n)Y_0(b\alpha_n) - J_0(b\alpha_n)Y_0(a\alpha_n)$

b/a	$a\alpha_1$	$a\alpha_2$	$a\alpha_3$	$a\alpha_4$	$a\alpha_5$
1.2	15.7014	31.4126	47.1217	62.8302	78.5385
1.5	6.2702	12.5598	18.8451	25.1294	31.4133
2.0	3.1230	6.2734	9.4182	12.5614	15.7040
2.5	2.0732	4.1773	6.2754	8.3717	10.4672
3.0	1.5485	3.1291	4.7038	6.2767	7.8487
3.5	1.2339	2.5002	3.7608	5.0196	6.2776
4.0	1.0244	2.0809	3.1322	4.1816	5.2301

2.4 Kinetics of Hydrogen Absorption and Desorption

Hirooka et al.(2000) proposed a method of reaction rate analysis in a constant volume system. This method is based on the assumption that the reaction rate reaches equilibrium. Thus, the hydrogen absorption and desorption rates are proportional to the difference between the hydrogen pressure, p, at time, t, and that at the equilibrium state, p_e .The reaction rate can be expressed by the rate of the hydrogen pressure change, dp/dt, due to the absorption or the desorption. Therefore, the rate equations for the absorption and the desorption are obtained:

$$-\frac{dp}{dt} = k_a(p - p_e) \tag{22}$$

$$\frac{dp}{dt} = k_d(p_e - p) \tag{23}$$

where k_a and k_d are the rate constants for absorption and desorption. These two equations are solved as follows:

$$\ln\left[\frac{p-p_e}{p_i-p_e}\right] = -k_a t \tag{24}$$

$$\ln\left[\frac{p_e-p}{p_e-p_i}\right] = -k_d t \tag{25}$$

where p_i is the initial hydrogen pressure. If the reaction fraction, F, is defined as $F = (p_i - p)/(p_i - p_e)$ for the absorption, or $F = (p - p_i/p_e - p_i)$ for the desorption, then a unified reaction equation for both absorption and desorption is obtained:

$$-\ln(1 - F) = kt \tag{26}$$

where k is the reaction rate constant which can be obtained from the experiment.

2.5 Hydrogen Permeation in Various metals and alloys

As the lightest of all elements, hydrogen in either molecular or atomic form must show rapid mass transport. The fact that hydrogen diffusion is so much larger than that of O, N and C in 15-20 orders of magnitude at room temperature is entirely due to the lower activation energies. The activation energies for hydrogen atom are about ten times smaller than O, N, and C (Volkl and Wipf, 1981).

The diffusion of gases through metals is referred to as physical diffusion when no reaction occurs between the metal and the gas. In chemical diffusion, a chemical reaction results in the formation or elimination of species (Mousavinejad, 2005).

Within a metal, the hydrogen molecules are dissociated and the hydrogen atoms occupy interstitial sites in the host metal lattice. A given interstitial site can be occupied only once. The hydrogen atoms can jump from one interstitial site to a neighboring vacant one, and can diffuse in this matter through the metal (Wipf, 2000).

When hydrogen is present in the bulk of the alloy, its transport is a simple process and is controlled by lattice diffusion. For an external environment, hydrogen transport can be controlled by any one of individual reaction steps indicated in Figure 2.8. The driving force for the diffusion is provided by gradients in concentration or from a gradient in the hydrostatic component of an elastic stress field (Oriani, 1994) or gradient in electric field or temperature (Manning, 1973). At temperatures below about 200°C, the diffusion is hindered by the traps (sites in the metal matrix) which capture and delay migrating hydrogen atoms (Dayal and Parvathavarthini, 2003).

There are several specific locations in a material where the presence of hydrogen may be critical to the fracture behavior. These include the lattice itself (hydrogen in solution) as well as grain boundaries, voids and dislocations as shown in Figure 2.9.

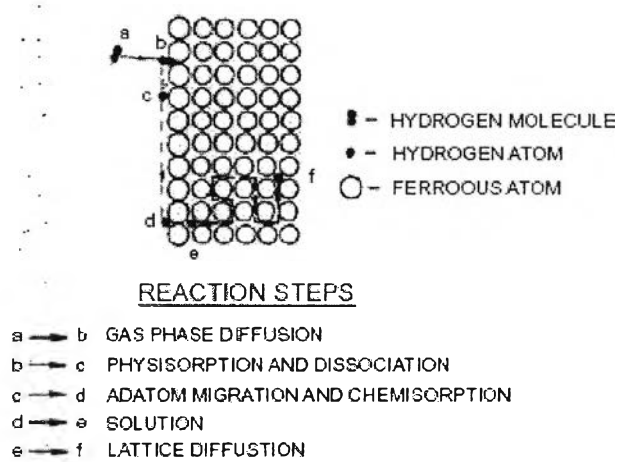

Figure 2.8 Schematic of possible reaction steps of external molecular hydrogen environment (Nelson, 1983).

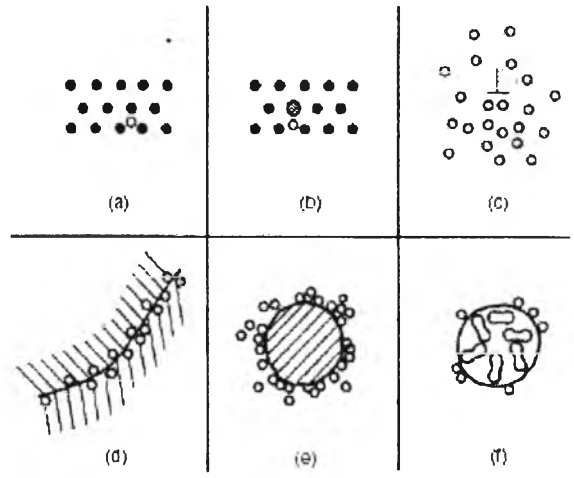

Figure 2.9 Schematic view of destination for hydrogen in a metal microstructure (a) Solid Solution; (b) Solute-hydrogen pair; (c) dislocation atmosphere; (d) grain boundary accumulation; (e) particle-matrix interface accumulation; (f) void containing recombined hydrogen (Thompson and Bernstein, 1980).

The diffusion laws are presented for the ideal case of diffusion without trapping. Due to its small volume, a hydrogen atom can diffuse and occupy the interstitial sites inside the material

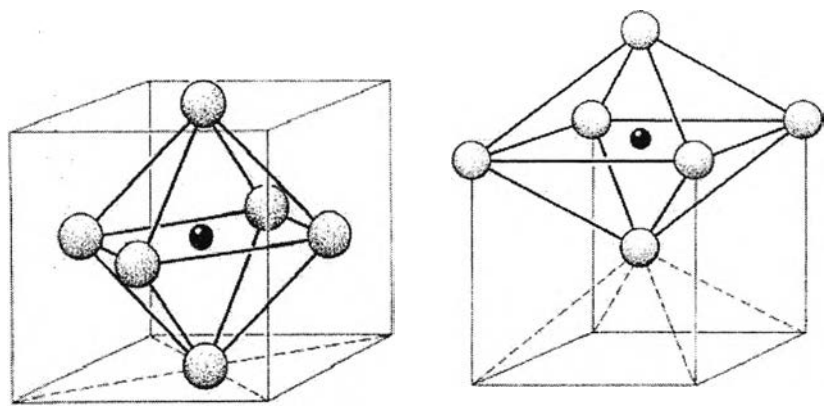

a) b)

Figure 2.10 Octahedral interstitial sites of face centered cubic (a) and body centered cubic (b) (Store, 2006).

The face-centered cubic (f.c.c.) lattice has one octahedral interstitial site per metal atom and two tetrahedral interstitial sites per metal atom in the unit cell.

The body-centered cubic (b.c.c.) lattice has three octahedral interstitial sites per metal atom and six tetrahedral interstitial sites per metal atom in the unit cell. In the f.c.c. lattice the octahedral positions (O) have the largest free volume, whereas in the b.c.c. lattice the tetrahedral sites (T) are the largest.

Table2.3 Interstitial sites occupied by hydrogen in different metals (Store, 2006)

Host lattice	Crystallographic structure	Occupied sites
α – Fe	b.c.c.	T
γ – Fe	f.c.c.	O
Pd	f.c.c.	O
Ta	b.c.c.	T
V	b.c.c.	T
Nb	Rhomb.	T

Hydrogen diffusion in steels is complicated because of the complex microstructure. The permeability of hydrogen through metallic membrane is a function of the lattice structure and various types of lattice and defects. Body Centered cubic (bcc) forms of Fe, V, Nb, and Ta commonly exhibit exceptionally high Hydrogen permeability. Face centered cubic (fcc) metals such as Pd also exhibit favorable hydrogen permeability. Many experiments have been reported on the hydrogen diffusivity through the metal membrane.

For the discussion of hydrogen permeation metals can be classified into three categories. Metals such as palladium and its alloys, especially with silver, have such high hydrogen permeability. Iron, nickel and their alloys have moderate hydrogen permeability. The last group is the least permeable metals, such as gold, tungsten and aluminum, which are often used to prevent hydrogen permeation (Lewis, 1967)

2.5.1 Iron

The diffusion of hydrogen in iron has been widely discussed in several reviews in term of the dependence of the diffusivity of hydrogen on temperature

based on the Arrhenius equation; $D = D_0 \exp(-E/RT)$. There are many studies on the diffusion coefficient of hydrogen dependence on temperature reported below:

Alefeld and VÖlkl (1978) proposed the equation for alpha iron,

$$D = 7.5 \times 10^{-8} \exp\left(\frac{-1{,}218.81}{T}\right) \quad cm^2 s^{-1} \qquad (27)$$

Salii et al. (1973) showed the diffusion coefficient as a function of temperature for pure alpha iron

$$D = 9 \times 10^{-8} \exp\left(\frac{-1{,}358.83}{T}\right) \quad cm^2 s^{-1} \qquad (28)$$

The diffusion coefficient of hydrogen dependence on temperature for the above equations gives different results. The possible reasons for variations are: surface processes, interaction of hydrogen with linear defects, and the development of micro-cracks and blisters in the metal as induced by hydrogen. The rate of hydrogen entry into the metal is much influenced by many variables such as its compositions, thermal-mechanical history, presence of a surface layer, presence of impurity, diffusion measuring method and pressure range of measurement (Matei, 1999).

2.5.2 Carbon Steel

Carbon steel is alloyed, singly or in combination, with chromium, nickel, copper, molybdenum, phosphorous and vanadium in the range of a few percent or less to produce low-alloy steels. The higher alloy additions are usually for better mechanical properties. The lower range of about 2% total maximum is of greater interest from the corrosion standpoint. Strengths are appreciably higher than carbon steel, but the most important is much better resistance to atmospheric corrosion.

Different types of carbon steel have different diffusion coefficients. The Table 2.4 shows previous studies of diffusion coefficient which measured the hydrogen through different types of carbon steel.

Kongvarhodom (2009) proposed the hydrogen diffusivity in carbon steel (ASTM A-179) as a function of temperature

$$D = 5.27 \times 10^{-9} exp\left(-\frac{9010.71}{RT}\right) \text{ m}^2\text{ s}^{-1} \quad (29)$$

Table 2.4 Hydrogen diffusivity through carbon steel

Types	Diffusion Coefficient(m^2/s)	Methods	References
Extremely low carbon steel	1.13×10^{-9} (25°C)	High sensitivity hydrogen microprint technique (HMT)	K.Ichitani and M. Kanno(2003)
Ultralow carbon steel	9.57×10^{-11}(25°C)	Electrochemical permeation technique	Xiaomin Yuan(2006)
Low carbon steel	3.82×10^{-12}(25°C)	Modification of the two-cell permeation technique	E.M.K Hillier and M.J. Robinson(2006)
Carbon steel X-65 (pipeline steel)	9.49×10^{-11}(25°C)	Time-to-breakthrough, Time lag, Fourier, and Laplace	Y.F.Cheng (2008)
Carbon steel ASTM A179	8.73×10^{-10}(310°C)	Reduction of pressure on a carbon steel tube membrane with time	C. Kongvarhodom (2009)

An example of this dependency is presented for carbon steel at different temperature. The flux is proportional to the surface concentration.

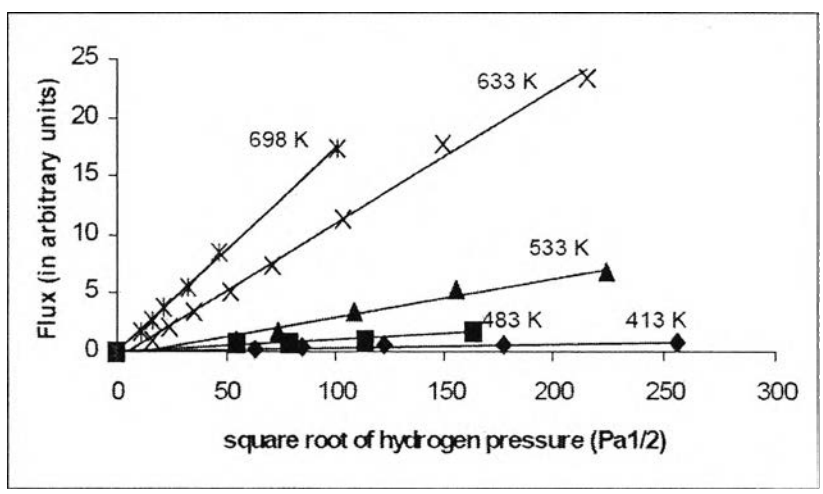

Figure 2.11 Hydrogen flux- hydrogen pressure dependency at different temperatures for carbon steels (Store, 2006).

2.5.3 Stainless Steel

Ferritic and austenitic groups of alloys are commonly used as structural materials in various engineering applications and are exposed in many instances to an aggressive chemical environment from which the hydrogen is introduced into the material.(Dayal and Parvathavarthini, 2003). Stainless steels which are austenitic alloys, owe their high resistance to corrosion in water and aqueous solutions at ambient temperature to the formation of a thin oxide layer. However, hydrogen diffusion in stainless steels has been found and these ferrous materials degraded resulting from hydrogen adsorption. The atomic model of hydrogen diffusion explains that hydrogen occupies interstitial sites in materials and diffuses by jumping from one interstitial site to another(Kumar and Balasubramaniam, 1997)

Previous works studied and also proposed the diffusion coefficient as a function of temperature as shown in the equations below

Louthan et al.(2004) used a hydrogen gas equilibrium method in the range of 100-450 °C. They reported the deuterium diffusion coefficient through 304 Stainless steel:

$$D = 4.7 \times 10^{-7} exp\left(-\frac{12900}{RT}\right) \ m^2 s^{-1} \quad (30)$$

Sun et al. (2004) showed the average diffusion coefficient of six alloys in a function of temperature. They performed the experiment in the temperature range 200-430 °C with 0.1 MPa of hydrogen pressure.

$$D = 5.7 \times 10^{-7} exp\left(-\frac{53620}{RT}\right) \ m^2 s^{-1} \quad (31)$$

Marchi and co-workers (2007) reported the diffusion coefficient of 300 series stainless steel in the function of temperature.

$$D = 8.9 \times 10^{-7} exp\left(-\frac{53900}{RT}\right) \ m^2 s^{-1} \quad (32)$$

Marchi et al. (2007) noted that The Fe-Cr-Ni-Mn stainless steels have a lower diffusivity of hydrogen and a higher solubility for hydrogen than 300-series stainless steels while permeability is the same for the two alloy group.

Forcey et al. (2004) reported permeability, diffusivity and sievert's constant of commercial 316L austenitic steel.

$$\text{Permeability}\left(mol\,m^{-1}s^{-1}Pa^{-\frac{1}{2}}\right) = 1.80 \times 10^{-7} exp\left(\frac{-64030}{RT}\right) \quad (33)$$

$$Diffusivity\ (m^2s^{-1}) = 3.82 \times 10^{-7} exp\left(\frac{-45500}{RT}\right) \quad (34)$$

$$\text{Sievert sconstant}\left(mol\,m^{-3}Pa^{-\frac{1}{2}}\right) = 1.50\ exp\left(\frac{-18510}{RT}\right) \quad (35)$$

2.5.4 Monel

Monel is a Ni-Cu based single-phase alloy. Monel exhibits excellent resistance to many corrosive environments. This alloy, unlike austenitic stainless steel, has been found to be resistant to chloride-induced stress cracking. Monel has been extensively used as a heat exchanger tube material. This alloy was employed as a SG tube material in early CANDU reactors(Dutta, 2009)

Meunier et al.(1981) performed the experiment by using Monel. The permeation of hydrogen was carried out between 550 and 700 K with a driving pressure of 20 bars and they proposed the diffusivity as the function of temperature of Monel .

$$D = 5.09 \times 10^{-7} exp\left(-\frac{5530}{T}\right)\ \text{m}^2\,\text{s}^{-1} \quad (36)$$

2.5.5 Palladium

Palladium has advantages as a coating because of its catalytic surface, high hydrogen permeability, infinite hydrogen selectivity, temperature stability, and corrosion resistance. Palladium exhibits high catalytic activity for the adsorption and dissociation of hydrogen into atoms entering the membrane and recombination of the atoms into molecular hydrogen exiting the membrane. The hydrogen permeability of

palladium increases with temperature because the endothermic activation energy for diffusion dominates the exothermic adsorption of hydrogen on palladium.

Diffusion of the hydrogen through the palladium is attributed to the "jumping" of hydrogen atoms through octahedral interstitial sites of the face-centered cubic palladium lattice. The lattice diffusion mode of mass transfer for hydrogen results in the essentially infinite selectivity of a palladium membrane (Morreale, Ciocco et al., 2003).

Völkl and Alefeld (1978) tabulated the diffusion coefficient data from many authors and used the Arrhenius equation to approximate the maximum diffusion coefficient (at infinite temperature) and the activation energy of diffusion for palladium

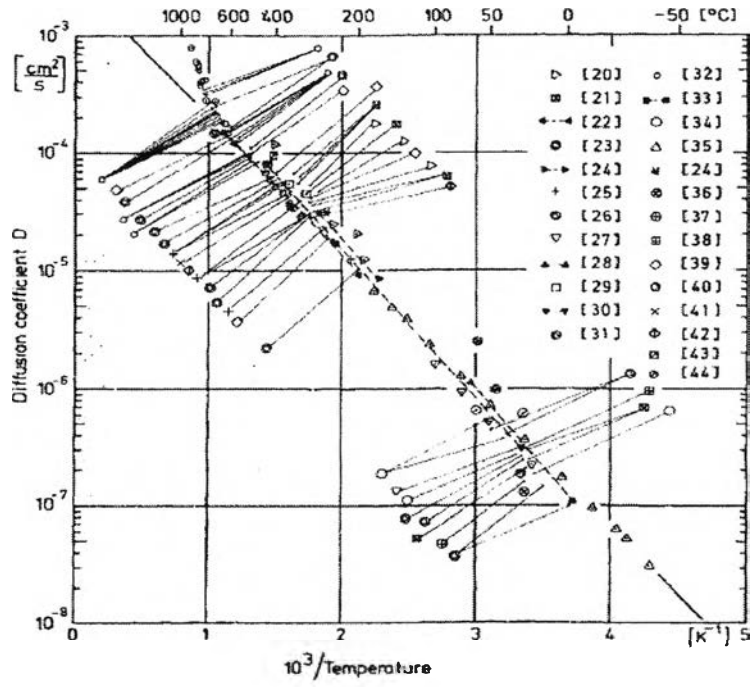

Figure 2.12 Diffusion coefficient of hydrogen in palladium (Aefeld and Volk, 1978).

They also proposed the diffusion coefficient as a function of temperature as shown in the equation below.

$$D = 2.9\times10^{-7}\exp\left(\frac{-22{,}196.47}{RT}\right)\ cm^2\,s^{-1} \qquad (37)$$

A hydrogen molecule is dissociated into two atoms on the metal surface, dissolves within the metal, diffuses through the metal atoms, and recombines

on the other side of the metal. An oxide film can form on the metal surface. The oxides have been proposed as diffusion barriers. Several studies showed that a noble metal could be used as a membrane to prevent oxide film formation. Palladium is one of materials that have high hydrogen selectivity for such a film.

Marchi and co-workers (2005) mentioned a palladium coating was applied to the oxide surface. The palladium catalyzes the dissociation of diatomic hydrogen eliminating the kinetic barrier at the surface and establishing conditions of diffusion-controlled transport of hydrogen. Bruzzoni et al. (2000) revealed the hydrogen coefficient increase when the exit surface is covered with a thin layer of Pd, which hinders the formation of an oxide film on this surface.

In Palladium the interstitial sites have octahedral symmetry, of which there is one site per Pd atom. These are the lower-energy sites so that these are preferentially be occupied by hydrogen. Hydrogen has a large mobility in transition metals especially in Pd (Oriani, 1994).

2.5.6 Platinum

Platinum is generally considered as both an inert metal which does not enter an electrochemical reaction and a catalytic metal that will provide the proper kinetics which increase the rate of chemical reactions (Ilic, Neuzil et al., 2000) .

Values of hydrogen solubility in platinum derived directly from gas/solid equilibrium measurements. These results are illustrated in Figure 2.13. The hydrogen solubility in platinum is lower values than palladium.

Ebisuzaki et al. (2000) have measured the hydrogen permeation in platinum. They used time lag technique to have the values of hydrogen diffusion coefficients. The relation is shown as the form:

$$D_{H_2} = 6.0 \times 10^{-5} \, exp\left(\frac{-5900 \; kcal}{RT}\right) \quad cm^2 s^{-1} \tag{38}$$

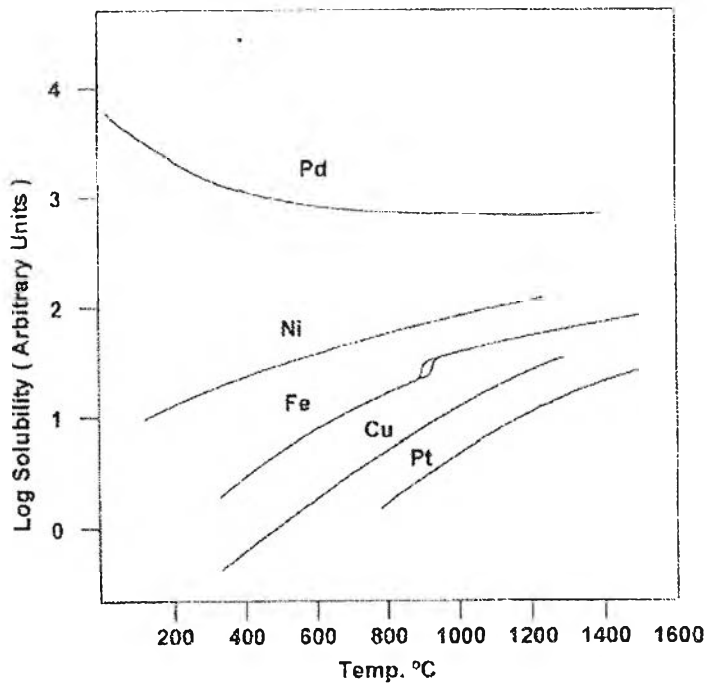

Figure 2.13 Schematic comparison of solubility of hydrogen in Group 8 metals at a pressure of 1 atm. Hydrogen Solubility as a function of temperature (Lewis, Kandasamy et al., 1967).

2.5.7 Copper

The diffusivity of hydrogen in copper at low temperatures using the electrochemical method was determined by Ishikawa and McClellan (1985). The hydrogen diffusivity in copper was measured in the temperature range 299-322.5K. The data at high temperatures from other investigators were subjected to a least-squares regression, and the resulting best-fit line is given by

$$D = 2.11 \times 10^{-6} \exp\left(\frac{-44{,}530}{RT}\right) \quad m^2 s^{-1} \qquad (39)$$

This hydrogen diffusivity is extrapolated to low temperatures that pass through the current results in this experiment and there are no deviations from classical Arrhenius diffusion behavior in the entire temperature range from 1200 down to 300K. Another determination of the dependence of diffusivity of hydrogen in copper on temperature at low temperatures was determined by Sakamoto and Takao who used the electrochemical permeation method. They found the following equation;

$$D = 3.69 \times 10^{-7} \exp\left(\frac{-36{,}820}{RT}\right) \quad m^2 s^{-1} \qquad (40)$$

2.6 Oxide Formation and Hydrogen Evolution

Many chemical and physical processes are controlled by the permeation, diffusion and solubility of gases in material. For example, metallurgists are concerned with the oxidation of metals via diffusion controlled processes, which often are controlled by surface oxide films, and with the diffusion of hydrogen and nitrogen into and through metals (Barrer, 1941) .

Exposure of metals and alloys to high temperatures leads to the formation of oxide scales. As the morphology of scale/substrate interface, oxidation of pure iron reveals three layers of scale. The innermost layer with the lowest oxygen content is wusite (FeO), with an intermediate magnetite (Fe_3O_4) layer and the outer scale hematite (Fe_2O_3). Sheasby and co-workers found the proportions of wusite, magnetite and hematite depend on temperature, materials and the media where the oxidation is carried out. It is reported that the dependence of scale thickness on time follows a logarithmic law when iron is oxidized in air at temperatures below 200°C. However, a parabolic dependence has been observed for nearly all metals in the intermediate temperatures of 250- 1200°C (Sun et al., 2004) .

The oxide film on carbon steel is magnetite (Fe_3O_4) which is a black and protective oxide. It is considered the most common oxide form on stainless steel at high temperatures and high pressures system (Basque, 1997). The metal oxide can act as a barrier for hydrogen transport. Thin passive or air-formed oxide films on iron impedes either hydrogen entry into the metal or hydrogen exit from the metal at room temperature.

When oxidized iron is contact with the gas phase, hydrogen entry takes place at a negligible or extremely low rate when exposed to hydrogen at room temperature with lower hydrogen pressure, whereas hydrogen exit is possible from the metal through the oxide to the gas phase. The presence of an oxide film impedes the inward

movement of hydrogen more than the outward movement (Bruzzoni and Riecke, 1994).

Hebaum and co-workers noted that surface oxides play a significant role in the hydrogen permeation behavior of steels. The presence of surface oxide could mask and/or distort the measured variables on hydrogen permeation and embrittlement. The oxide on the output side behaves as a catalytic recombination poisons such as As, Sn, Sb and other metalloids. This reduces the hydrogen permeation rate.

Schomberg (1996) used thick iron membranes in permeation experiments. Measurements were performed in a temperature range of 290-348 K. Some influence of the iron thickness was observed, indicating that both diffusion through the iron and through the oxide film limited the hydrogen permeation rate. Bruzzoni investigated the steady state hydrogen permeation through different oxide films thermally grown either in air or in oxygen at moderate temperatures (372-473). The activation energy for the hydrogen permeation coefficient of the oxide was estimated at 60-70 kJ mol^{-1}. The scatter in the measured values was attributed to an uncontrolled condition, for example, humidity during the thermal treatment and an uncontrolled surface roughness and high stresses produced by mechanical polishing. Time dependence was observed such that as the film was aged under continuous experimentation, it became less permeable to hydrogen.

Even the proposed mechanism of hydrogen transport through the iron oxide film was not clear, It can be concluded that the oxide film presents a definite resistance to the hydrogen steady state flow. This resistance depends on the temperature, film thickness and film composition. Bruzzoni and coworkers (2000) proposed the following equation to describe the hydrogen transport through an oxide film.

$$J_H = \frac{\sqrt{P_{H_2}}}{\left(\frac{L_{Fe}}{D_{H,Fe}} + R_{oxide}\right)} \tag{41}$$

where J_H is the flux of hydrogen, P_{H_2} is the partial pressure of hydrogen in system, L_{Fe} is distance of permeation, $D_{H,Fe}$ is hydrogen diffusion coefficient through the metal and R_{oxide} is oxide resistance.

Considering a model of simple hydrogen diffusion in oxide, the diffusion coefficients from the results of different researchers showed a range of 2×10^{-17} to 2×10^{-16} cm^{-2} s^{-1}.

The concentration profile within the metal phase should be linear, since the metal phase readily achieves steady state condition(Bruzzoni and Riecke,1994). Bruzzoni and co-workers presented the hydrogen concentration profile in Figure 2.14. The dotted line is for a Pd film at the input and output side of the metal membrane. The Pd film allowed equilibrium between the metal phase and the gas phase to be achieved. This is the maximum flow (J_{max}) for such membranes

$$J_{max} = D_{H,Fe}\frac{C^*}{L} \tag{42}$$

where C^* is a well defined value and depends only on temperature. If the oxide resistance at the exit surface is negligible, the steady state flow is limited only by the permeation coefficient of the metallic phase.

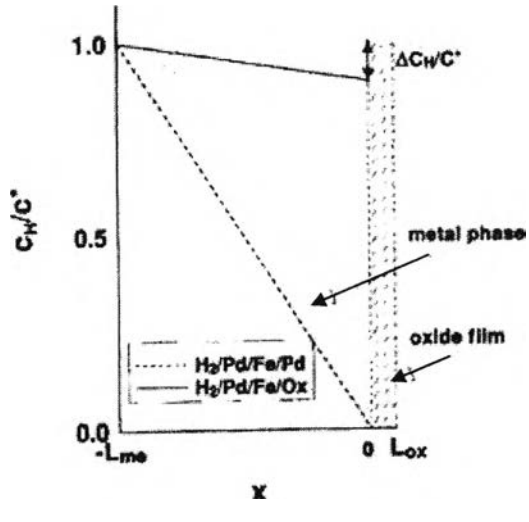

Figure 2.14 Sketch of the hydrogen concentration profile in the metal phase (Bruzzoni and Riecke, 1994).

In the presence of a layer metal oxide, the measured flow is much smaller than J_{max}. This means that the concentration drop in the metal phase is reduced. The conditions at the input surface are not changed but the output surface concentration of the metal is not zero. The equation for flux is obtained below:

$$J = D_{H,Fe}\frac{(C^*-C_H)}{L} \tag{43}$$

where C_H is the concentration at metal/oxide interface.

The structure, composition and the thickness of the passive film depend on the chemical composition of the alloy and the exposure conditions. For example, Stellwag revealed high chromium content stainless steels form Cr_2O_3. The Cr is added to Fe in an alloy to change the oxide film structure from polycrystalline to noncrystalline. The oxide film formed at high temperatures is orders of magnitude thicker than passive films grown at ambient temperature.

The oxide thickness was observed to exhibit a gradually decreasing growth rate with the exposure time according to approximate parabolic behavior (Bueno and Marino, 1999). The quasi-steady state hypothesis, which is used to simplify the mathematical analysis in diffusion systems where the diffusion path is changing slowly with time, applies to passive film growth. For this hypothesis to be valid, the rate of change of the diffusion path must be small, to allow for the concentration profiles to adjust to the changing situation(Bruzzoni and Riecke, 1994). However, some results showed that the passive film on steel was modified by hydrogen permeation.

Marchi et al (2007) proposed oxides acts as diffusion barriers for austenitic stainless steels in the wall of fusion reactors. These oxides, in some cases, have been shown to significantly reduce the apparent permeability. When these oxides are very thin, the oxide is thought to reduce the kinetics of diatomic hydrogen dissociation on the surface creating a process that is not rate-controlled by diffusion. They also noted that the permeability of hydrogen through steel is relatively unaffected by thick oxides; the interpretation being that once the oxide layer reaches a critical thickness the layers crack exposing metal surface. Moreover, high hydrogen pressure may result in reduction of the oxide and loss of the barrier effect. The apparent changes in hydrogen transport appear to be result of changing the rate-controlling step from lattice diffusion to a surface process such as adsorption and dissociation.

2.6.1 Reduction Iron Oxide by Hydrogen gas

Magnetite (Fe_3O_4) and Hematite (Fe_2O_3) are possible products on iron-based steel oxidation. Reduction of these proceeds in the steps below:

$$3Fe_2O_3 + H_2 \rightarrow 2Fe_3O_4 + H_2O \quad (44)$$

$$Fe_3O_4 + 4H_2 \rightarrow 3Fe + 4H_2O \quad (45)$$

$$(1-x)Fe_3O_4 + (1-4x)H_2 \rightarrow 3Fe_{(1-x)}O + (1-4x)H_2O \quad (46)$$

$$Fe_{(1-x)}O + H_2 \rightarrow (1-x)Fe + H_2O \quad (47)$$

The true fundamental trends of the different phase transformation steps during iron oxide reduction processes are Fe_2O_3–Fe_3O_4–FeO–Fe. It is important to note that the structural and morphological changes occurring at each of these stages caused by lattice construction and destruction of the primary texture. These changes on the macroscopic and microscopic scales have a direct bearing on the overall reduction kinetics (Bahgat and Khedr, 2007).

Piotrowski and co-workers (2005) presented the Avrami-Erofe'ev generalized method of comparing the kinetics of isothermal solid-state reactions. The method is based on the general equation describing nucleation and growth processes:

$$\alpha = 1 - \exp(-\beta t^m) \quad (48)$$

$$\ln(-ln(1-x)) = ln\beta + m \ln t \quad (49)$$

where α is the fraction reacted at time t (conversion degree for the time t), β is the constant, partially depending both on nucleation frequency and on rate of grain growth, and m is the constant associated with the geometry of the system. They performed experiments with mixtures of composition: 90% N_2 + 10% H_2. The experiment was carried out at 700-910°C. The results showed the time for total conversion of Fe_2O_3 into FeO shortens considerably with increasing temperature. Using H_2 in the mixture reduces the reduction reaction time from 27.45 to 4.18 min.

A literature survey indicates that the reduction rate of the oxide layer depends on the starting raw material, nature of the reducing gas, temperature range, reaction step, presence of water vapor in the gas mixture, impurities, physical shape, etc.

Table2.5 Suggested mathematical modeling of reaction kinetics (Pineau et al., 2007)

Equation	Shape Factor, F_p	Mechanism
$kt = 1 - (1 - X)^{\frac{1}{F_p}}$	1	General equation
$kt = 1 - (1 - X)^{1/2}$	2	Phase-boundary-controlled reaction (contracting cylinder)
$kt = X^2$	1	One-dimensional diffusion
$kt = X + (1 - X)\ln(1 - X)$	2	Two-dimensional diffusion
$kt = 1 - 3(1 - X)^{2/3} + 2(1 - X)$	3	Three-dimensional diffusion
$kt = [-\ln(1 - X)]$	1	Random nucleation; uni-molecule decay law (first-order)
$kt = [-\ln(1 - X)]^{1/2}$	2	Two-dimensional growth of nuclei (Avrami-Erofeyev equation)
$kt = [-\ln(1 - X)]^{1/3}$	3	Three-dimensional growth of nuclei (Avrami-Erofeyev equation)

where k is the constant, t is the reduction time (min), X is the extent of reduction (X=0 at the beginning of the reduction and X= 1 at the end of reduction and F_p is the particle shape factor (1 for infinites slabs, 2 for long cylinders and 3 for spheres)

Pineau et al. (1969) showed for the reduction of iron oxide with hydrogen in the temperature range of 200-680°C that the hematite was reduced to magnetite first. The reduction path of magnetite to iron is a function of the reaction temperature. At temperatures lower than 420°C, magnetite is reduced directly to iron. Mathematical modeling of experimental data suggests that the controlling mechanism is the two and three dimensional growth of nuclei and by phase boundary reaction at higher temperatures.